Hydrogenated Nanocrystalline Silicon *p*-Layer in *a*-Si:H *n-i-p* Solar Cells

Wenhui Du[a], Xianbo Liao[b], Xieshen Yang, Henry Povolny, Xianbi Xiang[b], Xunming Deng

Department of Physics and Astronomy, University of Toledo, Toledo, OH 43606, USA

K. Sun

Electron Microbeam Analysis Laboratory, University of Michigan, Ann Arbor, MI 48109, USA

This paper investigates the impacts of hydrogenated nanocrystalline silicon (*nc*-Si:H) *p*-layer on the photovoltaic parameters, especially the open circuit voltage (V_{oc}) of *n-i-p* type hydrogenated amorphous silicon (*a*-Si:H) solar cells. Raman scattering spectroscopy and transmission electron microscopy (TEM) analyses indicate that this p-layer is a diphasic material that contains nanocrystalline grains with size around 3-5 nm embedded in an amorphous silicon matrix. Optical transmission measurements show that the *nc*-Si *p*-layer has a wide bandgap of 1.96 eV, due to the quantum confinement effects (QCE). Using this kind of *p*-layer in *n-i-p a*-Si:H solar cells, the cell performances were improved with a V_{oc} of 1.042 V, while the solar cell deposited under a similar condition but incorporating a hydrogenated microcrystalline silicon (*µc*-Si:H) *p*-layer leads to a V_{oc} of 0.526 V.

---

[a] Electronic mail: wdu@physics.utoledo.edu
[b] Permanent address: Institute of Semiconductors, Chinese Academy of Sciences, Beijing 100083

The limiting factors of open circuit voltage of a-Si:H solar cells have been an interesting topic since a-Si:H alloys became a viable material for photovoltaic devices. Theoretical considerations expected that recombination originating from band tail states puts a fundamental limit on the output voltage of p-i-n a-Si:H solar cells, and the maximum V_{oc} calculated from the difference between the electron and hole quasi-Fermi levels in the intrinsic (i) layer is 1.0 ± 0.1 V.[1] Experimentally, using high hydrogen dilution or hydrogen-plasma treatment, a-Si:H solar cells with V_{oc} greater than 1.0 V could be fabricated,[2,3] which is well consistent with the above theoretical estimation.

However, it is noted that this estimate holds only for the situation when the built-in-potential in the i layer, set up by the doped (p and n) layers, is greater than the difference between the electron and hole quasi-Fermi levels. In fact, the doping layers, especially the p-layer acting as a window layer in both superstrate and substrate structures, have great influences on V_{oc} available in practical devices.

It was reported that using a μc-Si:H p-layer in a-Si:H n-i-p cells with a substrate structure on stainless steel (SS), the cell performance could be improved through an increase in the built-in potential of the junction and a decrease in the series resistance.[4] However, using a μc-Si:H p-layer in a-Si:H p-i-n cell with a superstrate structure on SnO_2 coated glass, it could induce a disastrous effect on the open circuit voltage and the fill factor (FF).[5] In a recent report, R. J. Koval et al argued that 10-20 nm thick p-layers prepared on i-layers under certain conditions may be amorphous even at hydrogen dilution values as high as 200, due to a possible barrier for microcrystal nucleation on an amorphous i-layer surface.[6] Moreover, they proposed that the maximum V_{oc} is obtained by incorporating p-type doped Si:H layers that are protocrystalline in nature, and even relatively low substrate-induced microcrystalline fractions in the p-layer are detrimental.[6]

The question is why the sue of a microcrystalline p-layer is detrimental for a-Si:H cell performances? An explanation was that this is due to the narrow bandgap (E_g) of μc-Si:H p-layer and a barrier at the p/i interface caused by the band offset between microcrystalline p-layer and amorphous i-layer.[5] This suggestion was confirmed by our simulation results,[7] using AMPS model developed at Penn State University.[8] Indeed, a "good" μc-Si:H p-layer with a large mean grain size (i.e., greater than 20 nm) and a large crystalline fraction should have a bandgap close to ~1.1 eV, the one of bulk crystalline silicon. However, if we could make a μc-Si:H p-layer with a wide bandgap, what will happen to the cells? And how can we make such a p-layer? One way to achieve a wide band gap p-layer is to use the QCE, i.e., to make μc-Si:H which comprise small Si nanocrystals embedded in an amorphous Si-H matrix. In this case the energy bangap of μc-Si:H should be enlarged by the QCE. In the following we prefer to use the term "nanocrystalline silicon", instead of "microcrystalline silicon" for such a kind of material. On the basis of the foregoing considerations it is appropriate in the present letter to identify the different effects of nc-Si:H and μc-Si:H p-layers on the performances of a-Si:H n-i-p cells.

The p-layer samples were prepared using conventional rf (13.56 MHz) PECVD and a gas mixture of SiH$_4$, BF$_3$ and H$_2$ in an ultrahigh-vacuum, multi-chamber, load-locked deposition system. For growing nc-Si:H p-layers we used a high hydrogen dilution (H$_2$/SiH$_4$=166) and a high gas pressure of 2 Torr as well as a high power density of 1.0 W/cm^2 at a low substrate temperature of 70°C. To increase microcrystallinity in the μc-Si p-layers, the deposition parameters were changed to a higher hydrogen dilution (H$_2$/SiH$_4$=200), a low gas pressure of 0.6 Torr as well as a low power density of 35mW/cm^2 at 200°C. Samples for use in a-Si:H n-i-p cells have a structure of SS/Al/ZnO/n-a-Si:H/i-a-Si:H/p-

Si:H/ITO, with a protocrystalline i-layer deposited using a gas mixture of Si_2H_6 and H_2 at a high hydrogen dilution (H_2/Si_2H_6=100) at 200^oC. To enhance the formation of nanocrystalline nucleation sites for the p-layer deposition, we inserted a seed layer between the p- and i-layer in the samples. For analyses of the optical and structural properties the p-layer samples were deposited on Corning 7059 glass using the identical conditions as used in the solar cells, but with different deposition times. The formation of silicon nanocrystals and their mean grain size in the samples were characterized by Raman scattering and TEM. In view of the fact that microcrystalline growth is sensitive to the substrate material and the accumulated thickness,[9] we also made a thin sub-seed and i-layer (15 nm) before the p-layer deposition on Corning 7059 glass, simulating the p/i interface structure of the cell samples, and took the Raman signals from both sides, the front surface and the back surface through the glass substrate.

The obtained Raman spectra for the nc-Si:H and μc-Si:H p-layer samples are given in Fig.1, which were recorded near backscattering geometry using an Ar+ laser operating at a wavelength of 488 nm and a double monochrometer in the silicon TO mode region. Curve (a) of Fig.1 shows the Raman spectrum of the μc-Si p-layer sample (~50 nm thick). This curve has a sharp peak at 521 cm^{-1}, which is typical for bulk crystalline Si. Curve (b) and (c) of Fig.1 are the spectra of the nc-Si:H p-layer sample (~350 nm thick), taken from the front surface and the back surface through the glass substrate, respectively. As generally observed with nc-Si:H, two peaks appear in the spectra, a broad peak at 480 cm^{-1}, which is characteristic of amorphous Si and a sharp peak at 514 cm^{-1}, which is characteristic of Si nanocrystals. It is seen that Curve (b) is dominated by the sharp peak at 514 cm^{-1}, while Curve (c) comprises a broad peak at 480 cm^{-1} and a small shoulder at ~514cm^{-1}, demonstrating the reported

dependence of crystallinity on the accumulated thickness.[9] The Gaussian deconvolution of the two Raman spectra data are listed in table 1, including the peak position (P_k), the peak area (A) of the TO modes and the volume crystalline fraction (C), which was determined using the ratio of peak area of crystalline to that of amorphous inclusions with a cross section ratio of 0.9.[10] As can be seen that the Raman spectrum taken from the backside shows a less volume crystalline fraction, although it has nearly the same Raman redshift of 7 cm^{-1} with respect to the TO phonon mode in bulk crystalline Si From this Raman redshift, we deduced the mean nanocrystal size to be 2.1 nm or 2.5 nm, according to a bond polarizability model of J. Zi *et al.*,[11] or a modified phonon confinement model of Campbell and Fauchet.[12,13] These estimated sizes might be smaller than the actual sizes, due to an overestimate of the phonon confinement effect without considering the existence of tensile stress in the film.[14]

In order to characterize the crystallization in a very thin *p*-layer, a JEOL 2010F STEM/TEM microscope was used. The films were lfted off from glass substrate by etching with a diluted HF solution and supported by a copper TEM grids. The thin *p*-layer sample has a hybrid, stacked structure, comprising a 15 nm thick *p*-layer on a 15 nm *i*-layer with a seed layer in between, which was deposited under identical conditions as those used in solar cells. Fig. 2(a) shows a high-angle annular dark-field (HAADF) image of the sample, where many separated bright dots were observed, which represent nanocrystalline particles. Most of the particles are ranging from 3 to 5 nm, larger than the estimated values from Raman study. Several large white dots in this figure are the clusters of 3 or 4 crystalline particles. In the insert a selected-area electron diffraction (SAED) is illustrated, indicating diffraction pattern with crystalline feature for the area probed. Fig. 2(b) shows a high-resolution electron microscopy (HREM) image, exhibiting the lattice image. The interference fringes separated by 0.31 nm correspond to the spacing of Si (111) planes of the nanocrystals. Fig. 2 (c) is a nano electron

diffraction (NED) taken from one of the bright dots indicating the crystalline nature of the particle. These images clearly demonstrate that the p-layer deposited at a low substrate temperature and a high hydrogen dilution contains nanocrystalline Si particles of 3-5 nm in size. We estimated the effective energy bandgap of these Si nanocrystals should be enlarged to 2.3-1.9 eV, if it is treated as isolated spherical quantum dots saturated with hydrogen, based on the density-function approach of B. Delley and E.F. Steigmeier.[15] In fact the optical transmittance measurements performed on the same nc-Si:H p-layer sample used in the Raman scattering (Fig. 1) show that its Tauc optical bandgap is about 1.96 eV, confirming that the nc-Si:H p-layer indeed possesses a wide bandgap. However, one could not simply compare the Tauc bandgap value with the above theoretical estimate, because the former is an effective bandgap width of a diphasic material with an indirect gap, while the latter is for isolated Si quantum dots.

Effectiveness of a thin nc-Si:H p-layer for a solar cell can be most convincingly judged in a cell configuration. We prepared n-i-p a-Si:H solar cells at a similar condition but using a nc-Si:H or μc-Si:H p-layer. The resultant typical I-V curves are demonstrated in Fig.3. It is observed that using a nc-Si:H p-layer the cell performances (Curve a) could be enhanced, with a V_{oc} of 1.042 V, a FF of 0.734, a short circuit current of 11.6 mA/cm^2, and an efficiency of 8.87 %, while incorporating a μc-Si:H p-layer into the cell (Curve b), the V_{oc} decreased to 0.526 V.

References

1. T. Tiedje, Appl. Phys. Lett. **40**, 627 (1982).

2. B.Yan, J. Yang, and S. Guha, Appl. Phys. Lett. **83**, 782 (2003).

3. S. Tsuge, Y. Hishikawa, S. Okamoto, M. Sasaki, S. Tsuda, S. Nakano, and Y. Kuwano, Mat. Rec. Soc. Symp. Proc. **258**, 869(1992).

4. S. Guha, J. Yang, P. Nath, and M. Hack, Appl. Phys. Lett. **49**, 218 (1986)

5. J. K. Rath, and R. E. I. Schropp, Solar Energy Materials and Solar Cells **53,** 189(1998).

6. R. J. Koval, Chi Chen, G. M. Ferreira, A. S. Ferlauto, J. M. Pearce, P. I. Rovira, C. R. Wronski, and R. W. Collinsa, Appl. Phys. Lett. **81**, 1258 (2002).

7. X. Liao, W. Wang and X. Deng, Proc. 29th IEEE-PVSC, 1234 (2002).

8. For AMPS, see http://www.psu.edu/dept/AMPS/.

9. Joohyun Koh, A. S. Ferlauto, P. I. Rovira, C. R. Wronski, and R. W. Collinsa, Appl. Phys. Lett. **75**, 2286 (1999)

10. G. Yue, J. D. Lorentzen, J. Lin, D. Han, and Q Wang, Appl. Phys. Lett. **75**, 492 (1999).

11. J. Zi, H. Buescher, C. Falter, W. Ludwig, K. Zhang and X. Xie, Appl. Phys. Lett. **69**, 200 (1996)

12. Ch. Ossadnika, S. Veprek, and I. Gregora, Thin Solid Films **337**, 148 (1999).

13. I. H. Campbell, P.M. Fauchet, Solid State Commun. **58**, 739 (1986).

14. V. Paillard, P. Puech, R. Sirvin, S. Hamma and P. Roca i Cabarrocas, J. Appl. Phys. **90**, 3276 (2001).

15. B. Delley and E.F. Steigmeier, Phys. Rev. **B 47**, 1397 (1997).

Figure and Table captions:

Figure1. Raman spectra of the μc-Si:H p-layer (Curve a) and the nc-Si:H p-layer samples taken from the front surface (Curve b) and the back surface (Curve c) through the glass substrate.

Figure 2. TEM micrographs of a thin nc-Si:H p-layer of 30 nm thick with a hybrid, stacked structure. (a) HAADF image, where bright dots represent nanocrystalline particles; in the insert is a SAED image, showing the diffraction pattern with crystalline features; (b) HREM image, exhibiting the lattice image; (c) NED image, indicating a formation of a crystal particle.

Figure 3. *I-V* characteristics of n-i-p a-Si:H solar cells on SS coated with Al/ZnO using the nc-Si:H p-layer (Curve a) or μc-Si:H p-layer (Curve b) as the window layer.

Table 1. Gaussion deconvolution of the Raman spectra of Curve (b) and Curve (c) in Fig.1, including the peak position (P_k) and the peak area (A) of the TO modes for crystalline (TO_c), amorphous (TO_a) and interfacial (TO_i) inclusions. The volume crystalline fraction (C) is also listed.
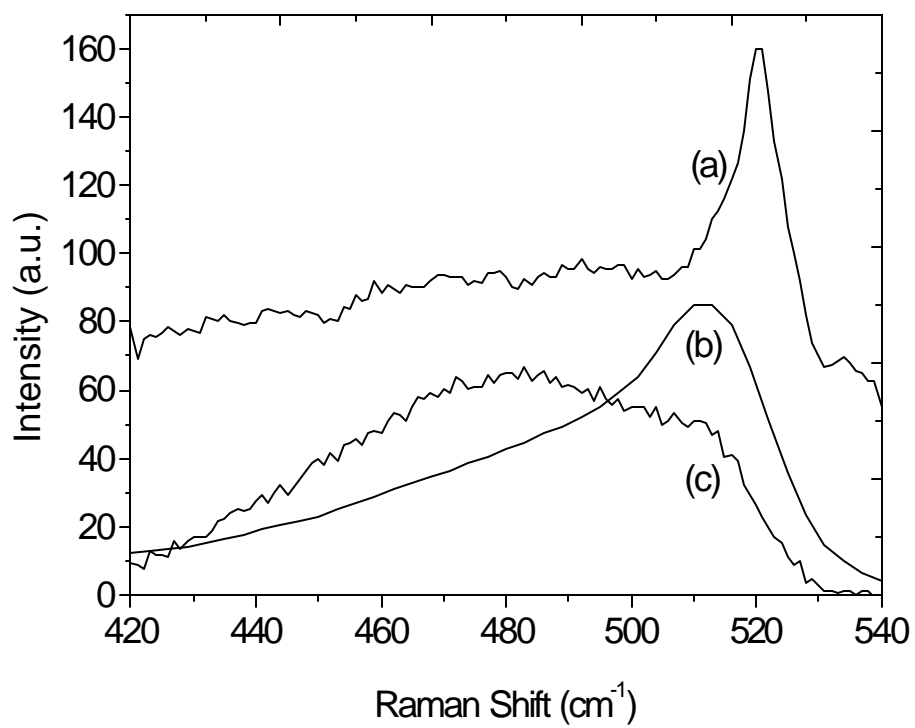
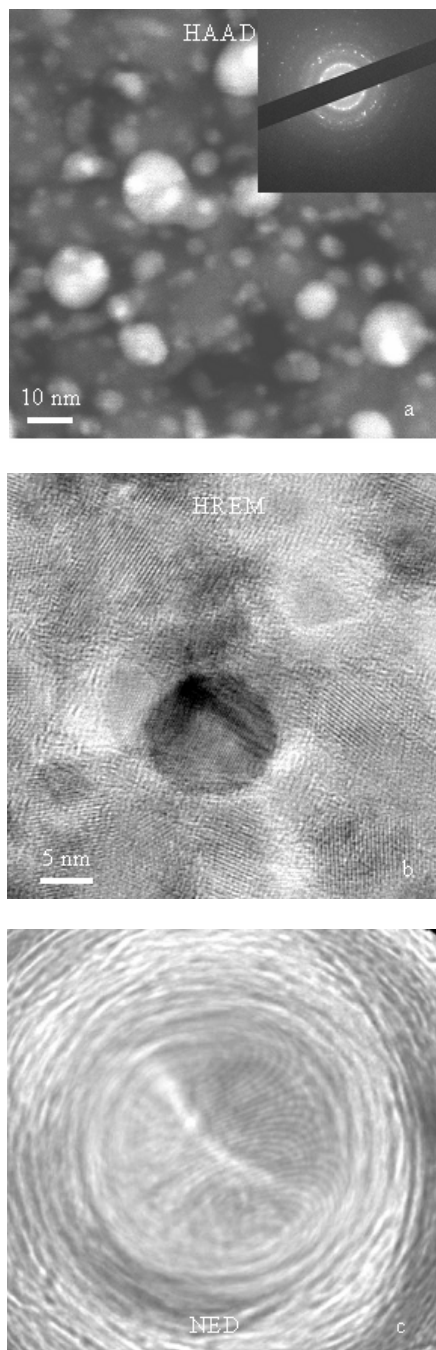Fig.1   Author: Wenhui Du et al.

Fig.2   Author: Wenhui Du et al.
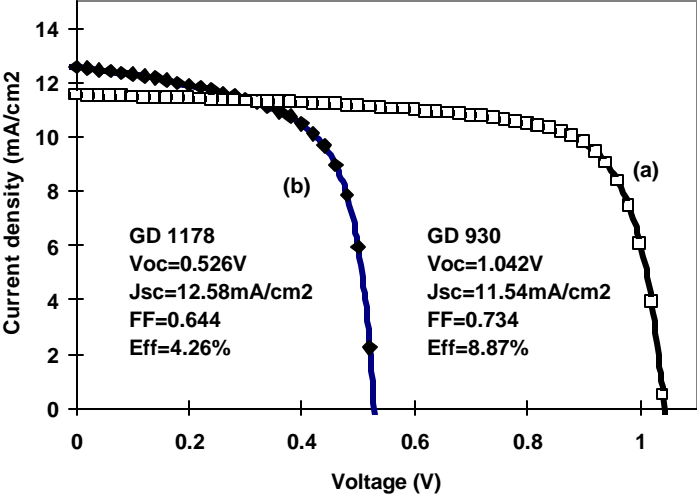
Fig.3   Author: Wenhui Du et al.

GD 1178
Voc=0.526V
Jsc=12.58mA/cm2
FF=0.644
Eff=4.26%

GD 930
Voc=1.042V
Jsc=11.54mA/cm2
FF=0.734
Eff=8.87%

(a)

(b)

Table 1

nc-Si p-layer	TOc		TOi		TOa		C
	Pk(cm^{-1})	A(a.u.)	Pk(cm^{-1})	A(a.u.)	Pk(cm^{-1})	A(a.u.)	
Top surface	514.2	87653	500.1	51031	480.2	194436	0.44
Back surface	514.0	52662	500.6	70339	480.3	228673	0.37